Hindawi Publishing Corporation
Journal of Metallurgy
Volume 2016, Article ID 6508597, 8 pages
http://dx.doi.org/10.1155/2016/6508597

Research Article

Bulk Mechanical Properties Testing of Metallic Marginal Glass Formers

Thien Q. Phan,[1] James P. Kelly,[2,3] Michael E. Kassner,[1,4] Veronica Eliasson,[1] Olivia A. Graeve,[2,3] and Andrea M. Hodge[1,4]

[1]*Department of Aerospace and Mechanical Engineering, University of Southern California, Olin Hall of Engineering 430, Los Angeles, CA 90089-1453, USA*
[2]*Department of Mechanical and Aerospace Engineering, University of California, San Diego, 9500 Gilman Drive, MC 0411, La Jolla, CA 92093-0411, USA*
[3]*Kazuo Inamori School of Engineering, Alfred University, 2 Pine Street, Alfred, NY 14802, USA*
[4]*Department of Chemical Engineering and Materials Science, University of Southern California, 925 Bloom Walk, HED 216, Los Angeles, CA 90089-1211, USA*

Correspondence should be addressed to Michael E. Kassner; kassner@usc.edu

Received 24 May 2016; Revised 22 July 2016; Accepted 26 July 2016

Academic Editor: Sunghak Lee

We developed a unique three-point bend testing apparatus to measure bulk mechanical properties of a model metallic glass alloy (SAM2X5 with nominal composition $Fe_{49.7}Cr_{17.1}Mn_{1.9}Mo_{7.4}W_{1.6}B_{15.2}C_{3.8}Si_{2.4}$) prepared by spark plasma sintering. The relatively large sample sizes in the present work allowed for the preparation of test specimens with a macroscale cross section (in the millimeter range) with well-controlled sample dimensions closer to standardized tests. Wire saw cutting allowed for a relatively sharp notch radius (3x smaller than previous studies) and minimal sample damage. We determined that Young's modulus and notch fracture toughness measured by our three-point bending apparatus are 230 GPa and 4.9 MPa·$m^{1/2}$. Also, Vickers indentation and flexure testing provided consistent results for Young's modulus. Indentation fracture toughness measured by Vickers indentation produced values at least 50% lower than by flexure. The microscale mechanical properties testing technique presented in this work and subsequent analyses are applicable to specimens of other compositions or ones prepared by other methods.

1. Introduction

Bulk metallic glasses (BMGs) generally have higher hardness and yield strength values compared to the crystalline forms of similar compositions [1–3]. However, low ductility and poor fracture toughness are often their main drawbacks; thus, efforts continue to be made to improve these properties [4–8]. This requires improvement in materials processing, as well as the development of accurate fracture toughness measurement techniques. While numerous methods to measure mechanical properties of macroscale samples exist, standard testing procedures are often impossible to implement for marginal metallic glass formers because processing limits the sample sizes that can be obtained of these materials. Spark plasma sintering [9–11] can overcome this sample size issue for some marginal glass formers so that macroscale properties can be measured [12–14].

Fracture toughness of Fe-based metallic glasses has been measured with indentation [15–17], whereas notch toughness testing has been completed on samples with nonstandard geometry [6, 18, 19]. Despite being most popular for samples with limited size, an indentation fracture test is not reliable for brittle materials because of the ill-defined crack arrest state that complicates analysis when compared to the rapid through-crack propagation of standardized tests [20, 21]. This results in serious discrepancies in mechanical properties data obtained by indentation. Consequently, it is more accurate to measure fracture toughness via a standardized technique like three-point bending.

However, three-point bend testing of metallic glasses may produce data that does not appear reliable. For example, previous fracture toughness measurements of Zr-based metallic glass obtained by three-point bending showed a large scatter in the data [20]. This is understood as a processing issue,

rather than a testing issue, and it is recognized that thermoplastic forming (such as spark plasma sintering) offers better control over sample thermal history to minimize processing-induced scatter [21]. Fracture toughness measurements of Fe-based metallic glasses have also been obtained by three-point bending [6, 18, 19], but the test specimens and notch were nonstandard geometries that can cause errors. Fracture toughness tests with notches machined using electric discharge machining (EDM) have been performed for metallic glasses [20, 22], but local heating caused by EDM can crystallize or even crack the volume of material in the heat-affected zone, which may lead to inaccurate fracture toughness values.

In the present work, methods to test Fe-based BMGs were devised to improve the accuracy of fracture toughness and modulus measurements of marginal glass formers. Spark plasma sintering was used to generate bulk samples of a model marginal glass former, SAM2X5 with nominal composition $Fe_{49.7}Cr_{17.1}Mn_{1.9}Mo_{7.4}W_{1.6}B_{15.2}C_{3.8}Si_{2.4}$. The relatively large sample size in the present work allowed for the preparation of test specimens with a macroscale cross section (in the millimeter range) with well-controlled sample dimensions closer to standardized tests. The larger size of the samples also allowed variations within a particular sample as well as amongst different samples to be investigated. Wire saw cutting allowed for a relatively sharp notch radius (3x smaller than previous studies) and minimal sample damage. These specimens were used in three-point bending for flexural modulus and fracture toughness tests using a custom-built mechanical testing apparatus. Given that values reported in this work is measured by a new technique, performed on a material processed by SPS, there is no directly comparable fracture toughness data. Thus, we tried to compare values measured by our new three-point bending technique to values that would be traditionally used to measure fracture toughness (such as indentation) on our material. Values for modulus and fracture toughness were also measured using indentation techniques (Vickers and nanoindentation) in order to compare with values measured using three-point bend tests. We used flexure and indentation results to calculate other properties and compare them to established properties. The microscale mechanical properties testing presented in this work and subsequent analyses are applicable to specimens of other compositions or ones prepared by other methods.

2. Experimental Procedures

Bulk SAM2X5 samples were produced using spark plasma sintering (SPS), as previously reported [12–14]. SAM2X5 powders were produced by gas atomization and were milled using a Fritsch P5 planetary high-energy ball mill. Size of the SAM2X5 powder particles is roughly 20 μm after milling. The sintering experiments on the powders were carried out with a Sumitomo SPS 1050 SPS unit (Sumitomo Coal Mining Co. Ltd., Japan) using 19 mm innerdiameter graphite dies lined with graphite paper, resulting in disks of ~2 mm thickness. The approximate amount of powder for each sample was 9 g. Sintering temperatures of 600°C were used and the applied load was 20 kN. The samples were cylindrical in shape with dimensions of 19 mm in diameter and 2 mm in thickness. SAM2X5 sample density was measured by an immersion technique. X-ray diffraction (XRD) patterns from a Rigaku Ultima IV system using CuKα radiation and a scan rate of 1° per second were used to assess the amorphous structure. XRD of the bulk samples was performed on the as-prepared, rough ground (400 grit), and diamond lapped discs to assess the effect of mechanical grinding and diamond lapping on sample crystallization. Transmission electron microscopy (TEM) imaging with SAED was performed using a JEM 2100F (JEOL) instrument on thin foil samples prepared by dimpling and ion-milling.

Two bulk X-ray amorphous SAM2X5 samples (Sample 1 and Sample 2) were selected for bend testing. Following our previous naming convention, our samples are designated SAM2X5-600 [12]. In order to mitigate the effects of heat and deformation, surface lapping and wire saw cutting were utilized due to their slow removal rates and low heat during implementation. The two samples were first lapped using diamond paste on both surfaces until the samples were 1860 μm in thickness and surfaces were parallel to within 1 μm over 20 mm. These samples were then cut into smaller specimens by a wire saw using a SiC slurry for modulus and fracture toughness tests. One of the bulk samples was cut into six flexural modulus specimens and four fracture toughness specimens and the other sample was cut into three flexural modulus specimens and three fracture toughness specimens.

Flexural modulus specimens were rectangular in shape and had cross sections of ~1860 μm × 500 μm in width and thickness, with test gauge lengths of 10 mm. Fracture toughness specimens followed ASTM E399 recommended ratios, however, specimens were about two times smaller than the standard size and have cross sections of ~1 mm × 1860 μm (width and thickness, resp.), and gauge lengths of 8 mm. Notching of the fracture toughness specimens was accomplished using a wiresaw, which used a 50 μm diameter wire and a cutting slurry composed of 800 grit SiC powder (suspended in oil) with a median particle size of 6.5 μm. The resulting notches were ~900 μm deep (about half the specimen thickness), were ~100 μm wide, and had notch root radii of ~40 μm, accurately measured using optical microscopy.

A small-scale mechanical testing apparatus (Figure 1) was custom designed and built to test the modulus and fracture toughness of millimeter scale specimens. The machine is similar to the testing apparatus used by Eberl et al. [23], which was used for testing thin films. Figure 1 illustrates the frame, two linear actuators, alignment stage, load cell, safety springs, and a camera. The actuators control stage movement and are controlled by Matlab software. The camera was used for digital image correlation (DIC) to monitor strain [23]. Fatigue precracks (as specified in ASTM E399) were not achieved due to early fracture. Therefore, toughness values reported are for notch toughness.

Indentation (Vickers and nanoindentation) was performed to compare to the modulus and toughness data obtained by bending tests. The samples were ground using 200, 400, 600, 800, and 1200 grit SiC paper and polished using a 1 μm diamond particle suspension. Vickers indentation was

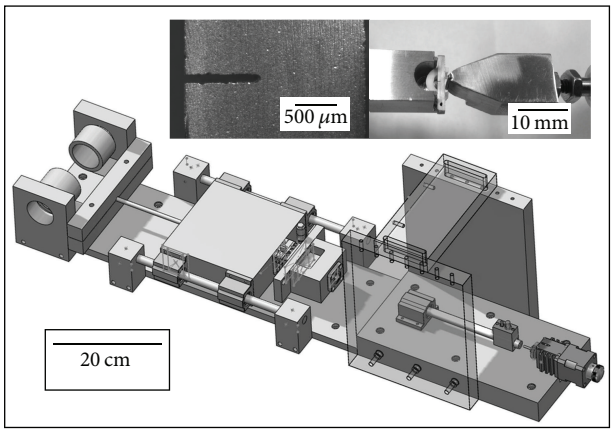

Figure 1: Microbending machine, close-up of fracture toughness stages, and sample.

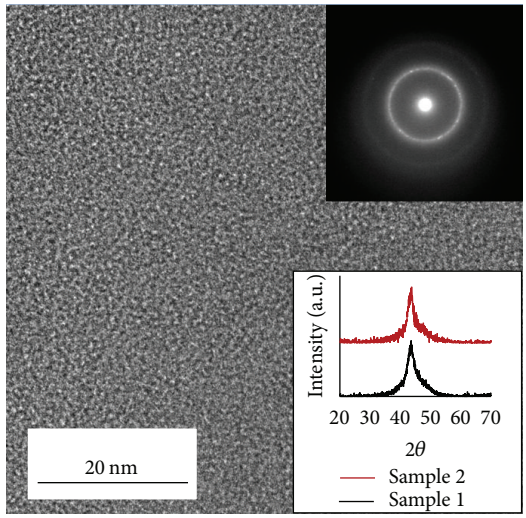

Figure 2: TEM image, inset SAED pattern, and inset XRD plots of SAM2X5 BMGs indicating amorphous morphology.

performed on the polished samples using a Leco LM100 indenter. For each sample, nine Vickers indentations were made using a load of 300 g and a dwell time of 10 s. Indentation toughness was calculated from the average of nine Vickers indents for each of the two bulk samples using optical measurements of the average crack lengths emanating from the indent corners. One of the most commonly used models to approximate fracture toughness of BMGs is that of Anstis et al. [24], where a half penny crack geometry is assumed and the indentation toughness can be estimated based on

$$K_c = \alpha \frac{P}{c_0^{3/2}} \sqrt{\frac{E}{H}}, \quad (1)$$

where K_c is the toughness calculated from indentation, α (0.016 ± 0.004) is the calibration constant (empirical constant), P is the indentation load, H is the hardness, E is the modulus, and c_0 is the half crack length.

Nanoindentations were made using a Hysitron Triboindenter and used to measure hardness and Young's modulus. A total of 36 nanoindents were made for each of the two bulk samples using a Berkovich tip (radius of 200 nm) with a constant loading rate of 1000 μN/s and a maximum load of 7500 μN. Hardness was calculated from the maximum force divided by the area function. Reduced modulus measured by nanoindentation was calculated based on the stiffness of the unloading curve and the area function. Young's modulus was then calculated from the reduced modulus (assuming $\upsilon = 0.3$).

Young's modulus measurements of the flexural specimens were performed using our three-point bending apparatus. The cross-head stage movement rate was 5 μm/s. Displacement values were determined from the movement of the piezo-actuator. Combined with the information from the load cell, a load-displacement curve was constructed for each modulus test, by subtracting the compliance of the machine that was separately measured. Young's modulus was calculated based on the beam bending theory for a supported prismatic beam with rectangular cross section using the following:

$$E = \frac{L^3 m}{4bd^3}, \quad (2)$$

where L is the length of the support, m is the slope of the load-displacement curve, b is the width of the specimen, and d is the thickness of the specimen. The machine and testing procedures were calibrated using an as-casted 6061-T6 Al specimen with a similar geometry to the SAM2X5 specimens. Young's modulus values measured from our testing device for 6061-T6 Al were within a 3% error of the accepted value of 69 GPa [25].

Figure 1 illustrates the top surface of the sample and the method by which it was loaded for fracture toughness measurements. The cross-head stage was moved at a rate of 2 μm/s for these measurements. Crack mouth opening displacement was tracked using DIC. A load versus crack mouth opening displacement curve was reconstructed by matching load cell data to DIC data. Recorded peak loads for each specimen were used to calculate fracture toughness following procedures in ASTM E399.

3. Results and Discussion

The bulk density of the SAM2X5-600 samples used in this study was 7.9 g/cm^3 and agrees well with our previous results that consider both the theoretical value for SAM2X5 powder (7.75 g/cm^3) and structural relaxation that occurs during the consolidation process [12–14]. The (identical) processing technique has been used in [12] to produce an amorphous alloy. Our previous study also demonstrates the microstructure of SAM2X5-600 and confirms a fully dense sample. The lower inset of Figure 2 illustrates XRD profiles of the samples. Figure 2 also illustrates the amorphous character of the SAM2X5-600 samples captured via bright field TEM.

The inset SAED pattern of the corresponding region shows diffuse rings with some diffraction spots. This suggests that the final material produced is not fully amorphous and has a combination of nanograin and amorphous structure. We did not quantitatively assess the percent volume of amorphous versus nanograin and suggest that the final sample is principally amorphous. Various sintering conditions (varying time and temperature) were used to synthesize the BMG samples. XRD results were used to determine the best sintering condition for the broadest diffraction peak with the least amount of crystalline peaks, which is at 600°C. Some crystallinity can be observed in the inset SAED pattern in Figure 2. However, this was the best that the authors could produce using SPS. Nevertheless, while the inclusion of crystalline particles can cause detrimental influence on toughness, it is important to measure the *global*, rather than *local* toughness of the material, since part life predictions depend on the global fracture toughness values. In using the three-point bending technique on larger specimens, the measured fracture toughness values take into account the "defects" such as crystallinity, which may be unavoidable in the synthesis of BMGs. This ensures that fracture toughness values measured via three-point bending would be usable in life predictions of parts made from our BMGs. Grinding and lapping did not change the XRD profiles, confirming that these specimen preparation procedures did not induce devitrification. Wire saw cutting is slower and produces less heat than rough grinding, so it is reasonable to infer that devitrification does not occur from this process either.

The average and first standard deviation of Young's modulus values measured by three-point bending are 227.3 ± 21.3 GPa for the six specimens prepared from Sample 1 and 232.3 ± 22.2 GPa from the three specimens prepared Sample 2. We take the average value as a good approximation of Young's modulus or 230 GPa. In comparison, the average and standard deviation of Young's modulus values obtained by nanoindentation are 276.5 ± 9.4 GPa and 303.3 ± 9.1 GPa. The results from nanoindentation are higher than those from three-point bending by about 20–30%. Average Vickers hardness values and standard deviations were 11.16±0.21 GPa and 12.21 ± 0.21 GPa. Vickers hardness can be used to estimate Young's modulus of metallic glasses ($E \cong 20\,\text{Hv}$) [26]. The estimated Young's modulus from the hardness values obtained by microindentation is 220 GPa to 240 GPa, which is in excellent agreement with the 230 GPa value obtained by our flexure tests. Alternatively, it is also possible to estimate Young's modulus from the weighted modulus of the alloy constituents [26]. Using this approach, Young's modulus for SAM2X5 is 300 GPa, which is in good agreement with our nanoindentation results. The calculations indicate that Vickers hardness is suitable for estimating Young's modulus of bulk materials, while the weighted Young's modulus using the alloy constituents provides a good estimate of Young's modulus obtained by nanoindentation. Average hardness values obtained by nanoindentation were 18.0 ± 0.51 GPa and 19.1 ± 0.46 GPa, which are higher than Vickers values. These hardness values do not reproduce Young's modulus results obtained by flexure when using the hardness relationship described above [26].

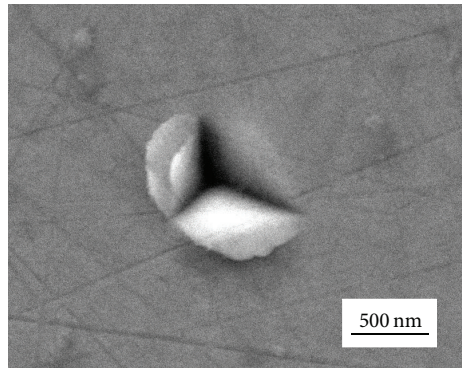

Figure 3: Nanoindent of SAM2X5. Material pile-up can be observed along the edges of the indent.

Figure 3 shows material pile-up along the edges of a nanoindent on our SAM2X5 sample. Material pile-up can overestimate Young's modulus and hardness measured by nanoindentation. Significant plasticity changes the effective contact area of the nanoindents so that the hardness can be overestimated by up to 50% [27]. Since nanoindentation exhibits pile-ups, the determination of the indent areas is difficult, and thus hardness values measured using nanoindentation are not precise. Thus, in retrospect, hardness values measured by Vickers indentation, with a higher load of 300 g, might be more representative. Given the 20–30% higher Young's modulus measured by nanoindentation, we estimate that the hardness is also 20–30% higher given the direct relationship between the modulus and hardness. Correcting for the 20–30% difference results in hardness values of 14 GPa to 15 GPa for Sample 1 and 15 GPa to 16 GPa for Sample 2. Using $E \cong 20H$ relationship with these corrected hardness values produces Young's moduli of approximately 280 GPa to 300 GPa and 290 GPa to 320 GPa, which is now consistent with the hardness results that were obtained from nanoindentation (276.5 ± 9.4 GPa and 303.3 ± 9.1 GPa).

Figure 4 shows a load-displacement curve for a flexural modulus test. All flexural modulus curves show an abrupt brittle failure. No significant plastic deformation was observed in any of the modulus test specimens. The glass transition temperature is also proportional to Young's modulus ($T_g = 2.5E$) (with T_g in Celsius and E in GPa) [26]. Using our measured Young's modulus by flexure or Vickers indentation (230 GPa) and $T_g = 2.5E$ relationship results in a glass transition temperature of 575°C, which is in excellent agreement with the reported glass transition temperature of 580°C for this material [28]. The glass transition temperature would be significantly overestimated by this method if using the direct nanoindentation results, justifying the use of our correction. Figure 4 (insert) shows a representative load versus crack mouth displacement curve for a fracture toughness test using three-point bending. All fracture toughness tests in this study exhibit no change in slope before failure with their load versus crack mouth displacement curves, consistent with brittle failure at the peak load. Average fracture toughness values measured by three-point bending are 5.0 ± 0.7 MPa·m$^{1/2}$

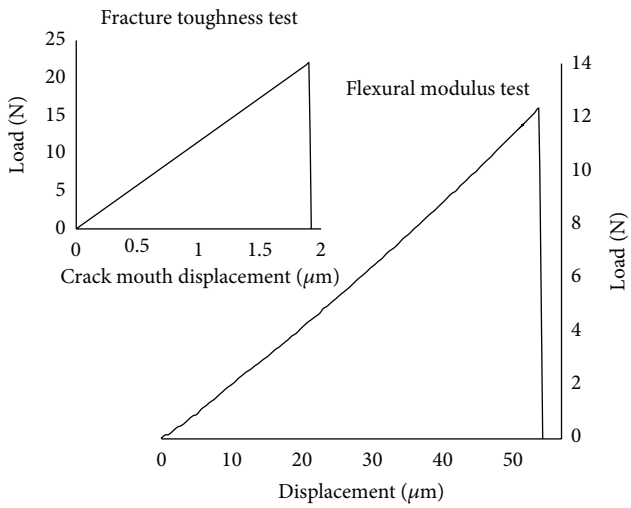

Figure 4: Flexural modulus and fracture toughness load versus displacement curves for SAM2X5 samples tested by three-point bending.

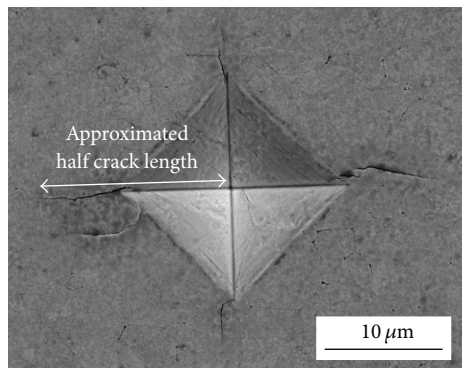

Figure 5: Fracture toughness measurements of half crack length using Vickers indentation. Cracks emanating from corners of Vickers indents are seldom straight nor symmetric about the center.

and 4.7 ± 0.8 MPa·m$^{1/2}$ for Sample 1 and Sample 2, respectively. There is insignificant difference between the two samples. Thus, we take an average value of 4.9 MPa·m$^{1/2}$ as the notch fracture toughness. Average indentation (Vickers) toughness values for both bulk samples are 2.5 ± 0.1 MPa·m$^{1/2}$ and 2.2 ± 0.1 MPa·m$^{1/2}$, respectively. It has been shown that FeB-based BMGs (SAM2X5) are stronger and more brittle than that of FeC and FeC(B)-based BMGs [29]. As expected, Vickers indentation toughness values reported for SAM2X5 (FeB-based BMG) are very slightly lower than for other FeC-based BMGs [15, 17]. However, Quinn and Bradt [30] point out that Vickers toughness values are unlikely to be accurate or valid, except fortuitously. Indeed, we find these values to be 50% lower than the values obtained by our three-point bend testing. Indentation toughness tests are burdened with a considerable amount of error [31]. For example, the assumed half penny crack geometries are often difficult to obtain, and the calculation does not account for the existence of irregular and secondary cracks (crack branching).

Figure 5 shows cracks emanating from a Vickers indent. The half crack length is measured optically as the distance from the center of the indent to the tip of the cracks. In using (1) to calculate fracture toughness, it is assumed that the cracks formed at the indent corners are straight and are equal in length. Cracks formed by Vickers indents in our SAM2X5 samples showed irregular cracks which add to errors in the calculated fracture toughness values. Vickers indentation determination of toughness is flawed with many issues, one of which is accurate determination of the crack lengths. This was the main driving force to develop the micromechanical tester to measure the toughness values more accurately. This is an issue not only in this study, but also in other studies measuring fracture toughness using indentation. Indentation fracture toughness values are only accurate to around ±40% based on work by Anstis et al. [24]. It is noted that the "calibration" constant (α) used in (1) is assumed to be material independent. In reality, this value is material dependent and is determined by comparison to accepted values obtained by bending tests. Thus fracture toughness measurement using Vickers indentation is only accurate if α is already determined, which is not the case for many BMGs where sample size prohibits bending tests. The accuracy of indentation results calculated using a standard "calibration" constant α (0.016) have been shown to deviate about 50% from standard ASTM K_{IC} measurements of SiC samples [30, 32].

It has been shown that sample size affects the mechanical properties in Zr-based BMGs. Conner et al. [33, 34] showed significant increase in bend ductility for Zr-based BMG wires and foils smaller than 1 mm in size. That is, plastic strain to fracture in bending increased significantly with decreasing sample size below a sample thickness of about 1 mm. Fracture toughness values obtained by three-point bending of specimens with dimensions of at least 1 mm are more comparable to values measured by large scale testing (per ASTM), and toughness values obtained by indentation are not representative of bulk properties.

Disparate results were reported on the effect of notched versus fatigue precracked specimens on the fracture toughness measurements of Zr-based BMGs. Toughness values of notched samples of various widths were reported to exhibit higher (2x) fracture toughness values compared to those of fatigue precracked samples [35, 36]. The discrepancy in toughness values was partly attributed to the differences in the failure mechanism at the notch root. The fatigue precracked samples in [35] had planar crack fronts, while notched samples exhibited large amounts of shear banding at the notch root as well as significant crack bifurcations. The authors posited that energy absorption from shear banding and crack bifurcations in notched samples may well explain the differences in measured toughness values. At the same time, others have also shown no noticeable difference in measured fracture toughness of notched versus fatigue precracked samples [20, 37] in Zr-based and Ti-based BMGs. In those studies, both the notched and fatigue precracked samples exhibited extreme ductility, revealing significant shear banding for both types of samples. Since failure mechanisms

for both types of samples were similar, energy absorption and thus measured toughness values were similar.

Currently, there has been no reported study comparing toughness values of notched versus fatigue precracked specimens (according to ASTM E399) for extremely brittle BMGs such as Fe-based BMGs. We failed to fatigue precrack the notched SAM2X5-600 specimens. However, notch toughness specimens tested in this present work all exhibited planar crack fronts and are absent of any shear banding or crack bifurcation, suggesting failure mechanisms similar to those of fatigue precracked specimens reported in [35] on Zr-based BMGs. Therefore, while fatigue precracks are lacking in toughness specimens for the present work, the manner in which cracks propagate suggests that notch toughness values would be consistent with toughness values for fatigue precracked SAM2X5 specimens.

The effect of notch root radius on fracture toughness of a fine-grained ceramic (with similar fracture toughness values to SAM2X5-600) was investigated by Nishida et al. [38]. Using a procedure similar to ours, sintered Al_2O_3 samples with grain size of 1 μm were tested using notches of various root radii (3 μm to 100 μm). The authors found that fracture toughness decreased with decreasing notch root radius to 10 μm, below which values were consistent. The difference between 40 μm root radius (as in the present study) and 10 μm root radius was about a 25% decrease, indicating that the notch toughness value we measured is probably overestimated. In the future, a small (sharp) notch root radius (approaching fatigue precrack) is desirable for fracture toughness measurements, as it is more accurate. Assuming a sharper root radius (i.e., less than 10 μm) would simulate a fatigue precrack and produce a value 25% lower than we measured. While fracture toughness depends on the size of the notch root radius, there appears to be a lower limit to this dependency. Results from sintered Al_2O_3 system show that, below 10 μm, values measured are identical. It is suggested that as long as the notch root radius is small enough to produce the same crack "system" as the fatigue precracked case, then fracture toughness values would be similar. Since fatigue precracks on the fracture toughness specimens could not be achieved, we ensured that the notch root radius was as small as possible. Planar crack fronts, absent of shear banding, are observed for our SAM2X5 specimens. Therefore, we believe that the values obtained by our three-point bending is close to the values obtained if the specimens were fatigue precracked. Using a much sharper notch, fracture toughness values using three-point bending *may* be lower, but by how much we cannot state with absolute certainty. However, using three-point bending, we have eliminated many sources of errors associated with Vickers indentation: ill-defined crack lengths and a calibration value which may result in values that differ in *either* direction of + or −40% of the "real" value. We know that the main source of error may be that of the notch root radius, which we tried to minimize as much as possible within reason. Since currently there is no way of measuring the absolute fracture toughness value of SPS SAM2X5, we believe that fracture toughness measured using our technique will give a more accurate value and we provided an estimate of how large the error and in which direction the real value may be. Thus, for other brittle bulk metallic glasses, it would be advantageous to use the technique presented in this paper for fracture toughness measurements.

4. Conclusions

Flexural modulus and fracture (notch) toughness for Fe-based bulk metallic glass were determined to be 230 GPa and 4.9 MPa·m$^{1/2}$, respectively. Flexural modulus values were lower than those measured by nanoindentation and more accurately represent bulk properties. Fracture toughness specimens and testing conditions were kept as close to ASTM E399 specifications as possible. Specimen sizes are roughly half the recommended values with all ratios as recommended. Measured notch toughness values of specimens without fatigue precracks (4.9 MPa·m$^{1/2}$) with relatively sharp notch root radii (40 μm) via three-point bending are more reliable than fracture toughness values measured by Vickers indents (50% lower). The observed differences between indentation measurements and three-point bending measurements are expected. Bulk fracture toughness and modulus measurements of BMGs using our new testing technique are more accurate compared with values measured by indentation due to large specimen size, specimen geometries (rectangular versus circular), and specimen preparations. Our larger specimen size is more likely to include inclusions and flaws within the material; thus, fracture toughness values measured are more representative of the bulk sample. Rectangular specimen geometries have constant cross section compared with cylindrical specimens, thus, fewer sources of measurement error of the crack tip. And finally, specimen preparations using wire saw cutting minimizes plasticity and thermal damage compared with EDM used by other laboratories, reducing the size of the damage layer.

Competing Interests

The authors declare that they have no competing interests.

Acknowledgments

Research was supported by the Defense Threat Reduction Agency Grant no. HDTRA1-11-1-0067. The authors would like to thank Professor Dr. Christoph Eberl at the University of Freiburg (Deputy Director at the Fraunhofer Institute for Mechanics of Materials) for help in the testing machine design and Matlab DIC software.

References

[1] T. Kozieł, A. Zielińska-Lipiec, J. Latuch, and S. Kąc, "Microstructure and properties of the in situ formed amorphous-crystalline composites in the Fe–Cu-based immiscible alloys," *Journal of Alloys and Compounds*, vol. 509, no. 14, pp. 4891–4895, 2011.

[2] C. Suryanarayana and A. Inoue, "Iron-based bulk metallic glasses," *International Materials Reviews*, vol. 58, no. 3, pp. 131–166, 2013.

[3] Z. P. Lu, C. T. Liu, J. R. Thompson, and W. D. Porter, "Structural amorphous steels," *Structural Amorphous Steels*, vol. 92, no. 24, Article ID 245503, 4 pages, 2004.

[4] X. Li, H. Kato, K. Yubuta, A. Makino, and A. Inoue, "Improved plasticity of iron-based high-strength bulk metallic glasses by copper-induced nanocrystallization," *Journal of Non-Crystalline Solids*, vol. 357, no. 15, pp. 3002–3005, 2011.

[5] K. Q. Qiu, J. Pang, Y. L. Ren, H. B. Zhang, C. L. Ma, and T. Zhang, "Fe-based bulk metallic glasses with a larger supercooled liquid region and high ductility," *Materials Science and Engineering A*, vol. 498, no. 1-2, pp. 464–467, 2008.

[6] J. J. Lewandowski, X. J. Gu, A. Shamimi Nouri, S. J. Poon, and G. J. Shiflet, "Tough Fe-based bulk metallic glasses," *Applied Physics Letters*, vol. 92, no. 9, Article ID 091918, 2008.

[7] K. F. Yao and C. Q. Zhang, "Fe-based bulk metallic glass with high plasticity," *Applied Physics Letters*, vol. 90, no. 6, Article ID 061901, 2007.

[8] S. F. Guo, L. Liu, N. Li, and Y. Li, "Fe-based bulk metallic glass matrix composite with large plasticity," *Scripta Materialia*, vol. 62, no. 6, pp. 329–332, 2010.

[9] J. P. Kelly and O. A. Graeve, "Mechanisms of pore formation in high-temperature carbides: case study of TaC prepared by spark plasma sintering," *Acta Materialia*, vol. 84, pp. 472–483, 2015.

[10] J. P. Kelly and O. A. Graeve, "Spark plasma sintering as an approach to manufacture bulk materials: feasibility and cost savings," *The Journal of The Minerals, Metals & Materials Society*, vol. 67, no. 1, pp. 29–33, 2015.

[11] K. Sinha, B. Pearson, S. R. Casolco, J. E. Garay, and O. A. Graeve, "Synthesis and consolidation of BaAl2Si2O 8:Eu: development of an integrated process for luminescent smart ceramic materials," *Journal of the American Ceramic Society*, vol. 92, no. 11, pp. 2504–2511, 2009.

[12] J. P. Kelly, S. M. Fuller, K. Seo et al., "Designing *in situ* and *ex situ* bulk metallic glass composites via spark plasma sintering in the super cooled liquid state," *Materials and Design*, vol. 93, pp. 26–38, 2016.

[13] O. A. Graeve, M. S. Saterlie, R. Kanakala, S. D. de la Torre, and J. C. Farmer, "The kinetics of devitrification of amorphous alloys: the time-temperature-crystallinity diagram describing the spark plasma sintering of Fe-based metallic glasses," *Scripta Materialia*, vol. 69, no. 2, pp. 143–148, 2013.

[14] O. A. Graeve, R. Kanakala, L. Kaufman et al., "Spark plasma sintering of Fe-based structural amorphous metals (SAM) with Y_2O_3 nanoparticle additions," *Materials Letters*, vol. 62, no. 17-18, pp. 2988–2991, 2008.

[15] V. Keryvin, X. D. Vu, V. H. Hoang, and J. Shen, "On the deformation morphology of bulk metallic glasses underneath a Vickers indentation," *Journal of Alloys and Compounds*, vol. 504, no. 1, pp. S41–S44, 2010.

[16] V. Keryvin, V. H. Hoang, and J. Shen, "Hardness, toughness, brittleness and cracking systems in an iron-based bulk metallic glass by indentation," *Intermetallics*, vol. 17, no. 4, pp. 211–217, 2009.

[17] P. A. Hess, S. J. Poon, G. J. Shiflet, and R. H. Dauskardt, "Indentation fracture toughness of amorphous steel," *Journal of Materials Research*, vol. 20, no. 4, pp. 783–786, 2005.

[18] S. F. Guo, K. C. Chan, and L. Liu, "Notch toughness of Fe-based bulk metallic glass and composites," *Journal of Alloys and Compounds*, vol. 509, no. 39, pp. 9441–9446, 2011.

[19] A. S. Nouri, X. J. Gu, S. J. Poon, G. J. Shiflet, and J. J. Lewandowski, "Chemistry (intrinsic) and inclusion (extrinsic) effects on the toughness and Weibull modulus of Fe-based bulk metallic glasses," *Philosophical Magazine Letters*, vol. 88, no. 11, pp. 853–861, 2008.

[20] A. Kawashima, H. Kurishita, H. Kimura, T. Zhang, and A. Inoue, "Fracture toughness of $Zr_{55}Al_{10}Ni_5Cu_{30}$ bulk metallic glass by 3-point bend testing," *Materials Transactions*, vol. 46, no. 7, pp. 1725–1732, 2005.

[21] W. Chen, J. Ketkaew, Z. Liu et al., "Does the fracture toughness of bulk metallic glasses scatter?" *Scripta Materialia*, vol. 107, pp. 1–4, 2015.

[22] R. L. Narayan, P. Tandaiya, G. R. Garrett, M. D. Demetriou, and U. Ramamurty, "On the variability in fracture toughness of 'ductile' bulk metallic glasses," *Scripta Materialia*, vol. 102, pp. 75–78, 2015.

[23] C. Eberl, D. S. Gianola, and K. J. Hemker, "Mechanical characterization of coatings using microbeam bending and digital image correlation techniques," *Experimental Mechanics*, vol. 50, no. 1, pp. 85–97, 2010.

[24] G. R. Anstis, P. Chantikul, B. R. Lawn, and D. B. Marshall, "A critical evaluation of indentation techniques for measuring fracture toughness. I, direct crack measurements," *Journal of the American Ceramic Society*, vol. 64, pp. 533–538, 1981.

[25] Aluminum Association, *Aluminum Standards & Data*, The Aluminum Association, New York, NY, USA, 1968.

[26] W. H. Wang, "The elastic properties, elastic models and elastic perspectives of metallic glasses," *Progress in Materials Science*, vol. 57, no. 3, pp. 487–656, 2012.

[27] W. C. Oliver and G. M. Pharr, "Measurement of hardness and elastic modulus by instrumented indentation: advances in understanding and refinements to methodology," *Journal of Materials Research*, vol. 19, no. 1, pp. 3–20, 2004.

[28] J. C. Farmer, J. J. Haslam, S. D. Day et al., "Corrosion resistance of thermally sprayed high-boron iron-based amorphous-metal coatings: $Fe_{49.7}Cr_{17.7}Mn_{1.9}Mo_{7.4}W_{1.6}B_{15.2}C_{3.8}Si_{2.4}$," *Journal of Materials Research*, vol. 22, no. 8, pp. 2297–2311, 2007.

[29] S. F. Guo, J. L. Qiu, P. Yu, S. H. Xie, and W. Chen, "Fe-based bulk metallic glasses: brittle or ductile?" *Applied Physics Letters*, vol. 105, no. 16, Article ID 161901, 2014.

[30] G. D. Quinn and R. C. Bradt, "On the vickers indentation fracture toughness test," *Journal of the American Ceramic Society*, vol. 90, no. 3, pp. 673–680, 2007.

[31] J. J. Kruzic, D. K. Kim, K. J. Koester, and R. O. Ritchie, "Indentation techniques for evaluating the fracture toughness of biomaterials and hard tissues," *Journal of the Mechanical Behavior of Biomedical Materials*, vol. 2, no. 4, pp. 384–395, 2009.

[32] Z. Li, A. Ghosh, A. S. Kobayashi, and R. C. Bradt, "Indentation fracture toughness of sintered silicon carbide in the Palmqvist crack regime," *Journal of the American Ceramic Society*, vol. 72, no. 6, pp. 904–911, 1989.

[33] R. D. Conner, W. L. Johnson, N. E. Paton, and W. D. Nix, "Shear bands and cracking of metallic glass plates in bending," *Journal of Applied Physics*, vol. 94, no. 2, pp. 904–911, 2003.

[34] R. D. Conner, Y. Li, W. D. Nix, and W. L. Johnson, "Shear band spacing under bending of Zr-based metallic glass plates," *Acta Materialia*, vol. 52, no. 8, pp. 2429–2434, 2004.

[35] P. Lowhaphandu and J. J. Lewandowski, "Fracture toughness and notched toughness of bulk amorphous alloy: Zr-Ti-Ni-Cu-Be," *Scripta Materialia*, vol. 38, no. 12, pp. 1811–1817, 1998.

[36] J. J. Lewandowski, A. K. Thurston, and P. Lowhaphandu, "Fracture toughness of amorphous metals and composites,"

Materials Research Society Symposium Proceedings, vol. 754, pp. 307–313, 2003.

[37] X. J. Gu, S. J. Poon, G. J. Shiflet, and J. J. Lewandowski, "Compressive plasticity and toughness of a Ti-based bulk metallic glass," *Acta Materialia*, vol. 58, no. 5, pp. 1708–1720, 2010.

[38] T. Nishida, Y. Hanaki, and G. Pezzotti, "Effect of notch-root radius on the fracture toughness of a fine-grained alumina," *Journal of the American Ceramic Society*, vol. 77, no. 2, pp. 606–608, 1994.